Journal Pre-proof

Cyanidin-3-*O*-glucoside Restores Spermatogenic Dysfunction in Cadmium-exposed Pubertal Mice *via* Histone Ubiquitination and Mitigating Oxidative Damage

Xusheng Li (Methodology) (Investigation) (Formal analysis)<ce:contributor-role>Writing-original draft), Zilan Yao<ce:contributor-role>Writing-original draft), Dacheng Yang (Validation) (Data curation), Xinwei Jiang (Methodology), Jianxia Sun (Visualization), Lingmin Tian (Resources), Biyu Wu<ce:contributor-role>Writing-review and editing), Weibin Bai (Conceptualization) (Supervision) (Project administration)

PII: S0304-3894(19)31660-7

DOI: https://doi.org/10.1016/j.jhazmat.2019.121706

Reference: HAZMAT 121706

To appear in: *Journal of Hazardous Materials*

Received Date: 15 September 2019

Revised Date: 14 November 2019

Accepted Date: 15 November 2019

Please cite this article as: Li X, Yao Z, Yang D, Jiang X, Sun J, Tian L, Wu B, Bai W, Cyanidin-3-*O*-glucoside Restores Spermatogenic Dysfunction in Cadmium-exposed Pubertal Mice *via* Histone Ubiquitination and Mitigating Oxidative Damage, *Journal of Hazardous Materials* (2019), doi: https://doi.org/10.1016/j.jhazmat.2019.121706

Cyanidin-3-*O*-glucoside Restores Spermatogenic Dysfunction in Cadmium-exposed Pubertal Mice *via* Histone Ubiquitination and Mitigating Oxidative Damage

Xusheng Li[a], Zilan Yao[a], Dacheng Yang[a], Xinwei Jiang[a], Jianxia Sun[b], Lingmin Tian[a], Biyu Wu[c], Weibin Bai[a,*] baiweibin@163.com

[a] Department of Food Science and Engineering, Institute of Food Safety and Nutrition, Guangdong Engineering Technology Center of Food Safety Molecular Rapid Detection, Jinan University, Guangzhou, 510632, PR China

[b] School of Chemical Engineering and Light Industry, Guangdong University of Technology, Guangzhou, 510006, PR China

[c] Department of Human, Nutrition, Food and Animal Science, University of Hawaii at Manoa, Honolulu, HI 96816, USA

[*] Address for correspondence: Weibin Bai, Ph.D., Department of Food Science and Engineering, Institute of Food Safety and Nutrition, Jinan University, 601 Huangpu Rd, Guangzhou 510632, PR China. 13822283521, +86-20-8522630

Graphical abstract

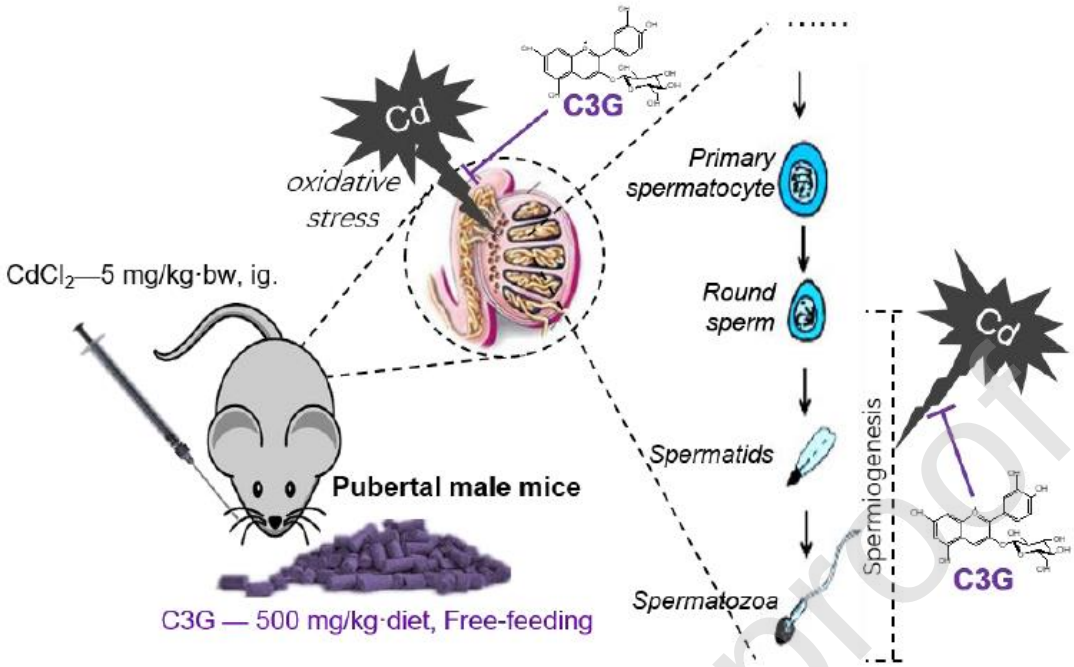

Highlights

- Cadmium causes spermiogenic defects at puberty, which differ from that at maturity.
- Consumption of C3G restores the declined semen quality caused by Cd.
- C3G normalizes histone modification for a smooth exchang of histone-to-protamine.
- C3G ameliorates the oxidative system of testes for reducing apoptosis of sperm cells.

Abstract: Cadmium (Cd) is an environmental contaminant found in soil, water, and food, and can cause oxidative stress and male reproductive damage. During puberty, the male reproductive system is very vulnerable to interference, however, the dysregulation of Cd on spermatogenesis in this period is ambiguous. The anthocyanin cyanidin-3-*O*-glucoside (C3G) is phytochemical rich in plants and fruits and has been shown to have remarkable anti-oxidant activity, making it an ideal nutrient for nutritional intervention. By modeling Cd-induced damage in male pubertal mice and feeding with C3G, we demonstrated that the C3G could rescue the amount and activity of sperm predominantly. Furthermore, C3G showed partial resistance to Cd-induced histone modification during spermiogenesis and prevented oxidative damage of the DNA in the sperm nucleus. Additionally, C3G mitigated the oxidative stress of testis to achieve the level coinciding with the control group. Meanwhile, Cd-induced mitochondrial apoptosis of sperm cells was reduced significantly *via* the MAPK signaling pathway in the presence of C3G. Collectively, our findings can offer a potential intervention for combating Cd-induced reproductive damage during puberty by taking anthocyanin as a dietary supplement.

Keywords: anthocyanin, cadmium, puberty, spermatogenesis, male infertility

1 Introduction

For the past forty years, males in multiple countries have experienced a reduction of more than 50% in the total number and concentration of semen. This reduction is partially responsible for approximately 15% of couples having failed pregnancy attempts

when participating in regular sexual intercourse [1,2]. Cadmium (Cd) is a heavy metal that is widely distributed in the environment and easily accessible through contaminated water, food, and air sources [3]. Cd can sustainably accumulate in the human body with a long half-life period of 20 to 40 years and has been considered a significant contributor of male infertility due to its serious reproductive toxicity [4]. In light of that, China is currently facing an increased risk of Cd exposure due to soil pollution [5], and the potentially harmful effects of Cd on reproduction has gained much interest.

Mounting epidemiological studies demonstrated that semen quality is inversely related to Cd levels in both the blood and semen [6-8]. Cd can interfere with sperm generation and maturation *via* multiple pathways. It is well documented that spermatogenic endothelium damage and blood-testis-barrier disruption are the primary targets of Cd in testis [9,10]. Moreover, Cd-induced oxidative stress, inflammation, and direct cytotoxicity to spermatogenic cells have also been considered factors that contribute to the failure of spermatogenesis in numerous studies [11-13]. Recently, accompanied by increasing epigenetic research on male infertility, the role that Cd plays in the abnormal histone modification of the sperm nucleus during spermiogenesis has become a major field of study. Spermiogenesis is a sophisticated biological stage that contributes to nucleosome remodeling, acrosome biogenesis, sperm tail biogenesis, and spermatid maturation [14,15]. Among these, histone modification is the initial step of the histone-to-protamine exchange in the sperm nucleus that is essential to proper nucleosome remodeling [14]. More importantly, *in vivo* evidence illustrates the negative influences from Cd on histone methylation [16] and acetylation [17]. This kind of abnormal histone modification can lead to incomplete histone-to-protamine exchange,

which disastrously gives rise to the failure of spermiogenesis and reduction in semen quality. These findings have advanced our understanding of how spermatogenesis is hindered by Cd. It is worth noting that existing research has demonstrated an age-dependent effect and a correlation with the methods of administration in Cd-induced male reproductive damage [13,18]. Therefore, testis at puberty with a higher sensitivity to exogenous contaminants may suffer diverse outcomes under oral exposure of chronic Cd that differs from testes that are sexually mature. This all should be considered with regard to the potential mechanisms and corresponding preventive measures.

Anthocyanin, a type of widely distributed flavonoid pigment, is commonly found in fruits, vegetables, and grains. Recently, the study of these compounds has increased because of its remarkable anti-oxidation and anti-inflammation capabilities [19]. Particularly, anthocyanin has the ability to attenuate Cd toxicity in various organs including the liver, kidney, and testis by alleviating oxidative stress, strengthening the anti-oxidative system, inhibiting inflammation, and chelating with Cd ion [18,20]. Cyanidin-3-O-glucoside (C3G) is the most typical and plentiful anthocyanin in the plant world. Our previous studies have revealed the protective effects of C3G against Cd-induced dysfunction of sex hormones *in vivo* and *in vitro* [18,21]. However, its ability in terms of guarding spermatogenesis still remains unknown.

In the present study, we sought to examine whether C3G could protect against Cd-induced male reproductive toxicity and spermatogenesis disturbances. We modeled male reproductive damage in mice by gavage cadmium chloride in order to be consistent with reasonable human Cd exposure and supplemented the highly purified

C3G in the diet.

2 Methods

2.1 C3G Preparation and Purification

Black soybean peels, the raw material for C3G preparation, were obtained from Anhui province, China. The acquisition of anthocyanin crude extracts from black soybean peels was in accordance with the methods as described in our previous study [18]. Next, the high-purity C3G was isolated from the anthocyanin crude extracts by preparative medium pressure liquid chromatography [22]. As shown in Supplementary Figure 1, the chemical structure of the isolated compound was identified as C3G *via* the molecular mass from HPLC-MS/MS, and the purity was 91.46% after peak area normalization.

2.2 Reagent and Antibodies

Primary antibodies for 8-hydroxy-2'deoxyguanosine (8-OHdG), Histone H2A, Histone H2B, and N-cadherin were purchased from Abcam (Cambridge, UK). Antibodies for acetyl-Histone H4 at lysine site 5, 8 and 12 respectively, B-cell lymphoma 2 (Bcl-2), Cleaved-Cysteine-aspartic proteases 3 (Cleaved-Caspase 3), Histone H4, phospho-P38 mitogen-activated protein kinases (p-p38) were obtained from Affinity (Cincinnati, USA). Antibodies for Bcl-2-associated death promoter (Bad), Bcl-2-associated X protein (Bax), Cleaved-poly ADP-ribose polymerase (Cleaved-PARP), Extracellular signal-regulated kinase (ERK), Glyceraldehyde-3-phosphate dehydrogenase (GAPDH), c-Jun N-terminal kinase (JNK), p38, p-ERK, p-JNK, ubiquitin-H2A, ubiquitin-H2B were purchased from

Cell Signaling Technology (Boston, USA). Antibodies for Caspase 3, Full PARP, p53, Zonula occludens-1 (ZO-1) were from Proteintech (Wuhan, China). Anti-phospho-p53 was from Bioss (Beijing, China), and anti-Occludin was from Invitrogen (Carlsbad, USA). The secondary anti-rabbit IgG antibody and anti-mouse IgG antibody were from Cell Signaling Technology and Proteintech respectively. The analytical grade of cadmium chloride was from Sigma-Aldrich (MO, USA). All other chemicals in this study were of analytical grade unless otherwise noted.

2.3 Animals and Treatment

The animal study authorized by the Animal Care and Protection Committee of Jinan University was carried out according to the guidance and recommendations of the Care and Use of Laboratory Animals. Ninety-six male Kunming mice (3 weeks old) were obtained from Guangdong Medical Laboratory Animal Center (Guangzhou, China). The animals were allowed access to chow and water *ad libitum* and maintained at 23℃ with 12/12-h light-dark cycle. All mice were randomly divided into three groups after acclimatization for 4 days: the control group (standard chow plus vehicle *via* gavage), the Cd-treated group (standard chow plus 5 mg/kg/day cadmium chloride dissolved in normal saline *via* gavage), and the Cd plus C3G (500 mg/kg C3G with chow plus cadmium chloride *via* gavage) group. Eight, eight, and twelve mice of each group were sacrificed at days 10, 20 and 30, respectively. Additionally, the remaining 4 mice in each group were sacrificed without any treatment at the beginning of the experiment period to serve as the basic control. After mice were narcotized and anogenital distance was measured, the blood was separated by extirpating eyeballs. The left cauda epididymis

was removed immediately for semen analysis and the left testis was stored at -80℃ until the determination of protein, mRNA expression, and other parameters. The right testis and right epididymis were respectively fixed in modified Davidson's fluid and 4% paraformaldehyde for further histological analysis.

2.4 Semen Analysis

The left cauda epididymis was put into 1 mL DMEM medium at 37℃ and simultaneously cut into small pieces for an entire sperm releasing at a sustaining temperature of 37℃ for 30 min. The sperm suspension was analyzed by a computer-aided semen analysis system (CASA, Song Jing Tian Lun Biotechnology Co., Ltd., Nanning, China). At least 30 fields each mouse were captured and the index including sperm concentration, mobility, vitality, abnormality, and other motion parameters was examined for a comprehensive assessment.

2.5 Histology and Spermatogenic Tubules Score

All fixed testis and epididymis were embedded in paraffin and sectioned into slides with a thickness of 5 μm. Then the slides were stained by hematoxylin and eosin (H&E) followed by a conventional protocol for morphological observation. Testis slides also were stained with Periodic acid-Schiff's (PAS) reagent for determination of stages of seminiferous epithelium cycles, thereby the ratios between spermatids and Sertoli cells at different steps were shown according to the presentation of PAS staining. For evaluating the changes of seminiferous epithelium, the spermatogenic tubules score was conducted according to the standard of testicular modified Johnsen score as

described previously [23]. At least 50 spermatogenic tubules were analyzed in each mouse for an accurate and representative evaluation.

2.6 Immunohistochemistry and Immunofluorescence

Immunohistochemistry was performed on 5 μm testis paraffin sections using a standard procedure essentially as previously described [22] with the following primary antibodies: anti-Histone H2A, anti-Histone H2B, anti-ub-H2A, anti-ub-H2B. For the immunofluorescence staining, the testis sections were put into a citrate buffer for antigen retrieving by microwave. After blocking nonspecific sites with 3% bovine serum albumin (BSA) for 5 min, the sections were incubated with primary antibodies to N-cadherin, ZO-1, Occludin or 8-OHdG overnight at 4℃, and suitably labeled fluorescent secondary antibodies. Subsequently, DAPI was used for nuclear staining for 5 min and images were collected immediately using a fluorescence microscope (Nikon, Japan) at corresponding detection wavelength.

2.7 TUNEL Assay

Apoptosis of cells was evaluated in testis sections using a terminal-deoxynucleotidyl transferase-mediated nick end labeling (TUNEL) staining in accordance with the manufacturer's manual of the assay kit from Beyotime Biotech (Shanghai, China).

2.8 Measurements of Enzyme and Oxidative Stress Markers

Testis homogenates were prepared for determination of superoxide dismutase (SOD), glutathione (GSH/GSSG) and malondialdehyde (MDA) according to commercial kit's

protocol (Jiancheng Biotech, Nanjing, China). The level of histone deacetylase (HDAC) and histone acetyltransferase (HAT) in the testis was measured using a commercialized enzyme-linked immunosorbent assay (ELISA) kit from Meimian Biotech (Yangcheng, China) following the manufacturer's instructions.

2.9 Protein Extraction and Western Blot

Dissected testis was homogenized with RIPA lysis buffer containing a cocktail of protease inhibitors and phenylmethanesulfonyl fluoride (PMSF). Afterward, the supernatant was collected after centrifugation at 14000 g for 10 min at 4℃, meanwhile, the protein concentration was measured by BCA Protein Assay kit (Beyotime Biotech). Then, 2.0 μg/μL of protein samples for separation was prepared with PBS and protein loading buffer. Total 20 μg protein in each sample were fractionated by sodium dodecyl sulfate-polyacrylamide gel (SDS-PAGE) and electrophoretically transferred onto a PVDF membrane. Samples were subjected to Western blot analysis following the standard protocol conducted in our previous research probed with antibodies for H2A, H2B, H4, acetyl-H4 (Lys5), acetyl-H4 (Lys8), acetyl-H4 (Lys12), ERK, p-ERK, JNK, p-JNK, p38, p-p38, p53, p-p53, Bax, Bcl-2, Bad, caspase 3, Cleaved-caspase 3, Full PARP, or Cleaved-PARP, respectively.

2.10 RNA Extraction and Gene Expression Assays

Total RNA was prepared from testis tissue with Trizol reagent following the manufacturer's protocol and converted to complementary DNA (cDNA) by using a high capacity cDNA reverse transcription kit (TaKaRa, RR047A, Japan). Quantitative real-

time PCR was performed by using TB Green Premix Ex Taq II (TaKaRa, RR820A). Amplification was conducted in a 20 μL reaction volume using a CFX96 real-time PCR detection system (Bio-Rad) with the process of which initiated at 95 °C for 30 s, followed by 5 s at 95 °C (40 cycles) for denaturation, and then annealing for 30 s at 60 °C. Primer sequences used in this study are provided in Table 1.

2.11 Statistical Analysis

SPSS 22.0 (SPSS Inc., Chicago, USA) was used for statistical analysis and GraphPad Prism 8.0 (San Diego, USA) was used for graph presentation. Data involved in the testicular score and sperm parameters were performed as median with range, and the corresponding significance of difference was analyzed by the Kruskal-Wallis Test. All other data were expressed as mean±standard deviation (SD), and the differences between all groups were conducted by one-way analysis of variance (ANOVA) with Tukey's multiple comparisons test as the post-hoc comparison. The value of $p \leq 0.05$ was considered to be statistically significant.

3 Results

3.1 Effects of C3G on Testicular Weight and Sperms Quality in Cd-exposed Mice.

Pubertal mice with Cd-induced spermatogenesis dysfunction was utilized and treated for 30 days until the mice reached sexual maturity. The testis and epididymis of mice were removed immediately and weighed post sacrifice at the specified time points. As shown in Table 2, the testis weight and anogenital distance of mice from the Cd group were decreased after treatment for 30 days, and the nutritional intervention with C3G

mitigated this damage predominately. However, there was no significant difference with regard to testis index, epididymis weight, and epididymis index between all three groups (Table 2). Most importantly and excitingly, the semen analysis by CASA system demonstrated that C3G treatment can elevate the decreased sperm counts (Figure 1 A-B), sperm motility (Figure 1 C) and vitality (Figure 1 D) caused by Cd significantly. Equally, there is also a positive effect of C3G on the other motion parameters of sperms suggesting that the motor ability of the sperm was protected from the Cd-induced sperm damage (Table 3). However, the abnormal sperm rate in this study was not disturbed by both Cd and C3G (Figure 1 E). Furthermore, the C3G treatment alone caused no apparent change in the healthy condition of sperms in our previous study (Supplementary Figure 2).

3.2 Effects of C3G on Cd-induced Spermiogenesis Damage.

Notably, the exposure condition used in this study of 5.0 mg/kg.bw $CdCl_2$ during male puberty for 30 days caused no histological structural changes of the spermatogenic tubule (Figure 2 A). The construction of the BTB was also assessed, and the results indicated an integrated BTB structure after Cd exposure (Supplementary Figure 3). This was contradictory to what others have published on Cd exposure in mice and rats. Together, this discrepancy of this phenotypic characteristic may be from the age-dependent effects and different methods of administration used in the present study.

H&E staining of the testis from the Cd group exhibited an emptier lumen of seminiferous tubule and a lower density of sperms in the cauda epididymidis (Figure 2 A-B). Simultaneously, PAS staining was conducted for a comprehensive spermatogenic

epithelium analysis (Figure 3 A). The Johnsen's Score of the seminiferous epithelium was reduced significantly after Cd exposure (Figure 3 B). Interestingly, the C3G intervention group exhibited a normal testis as seen by increased score and a perfect cauda epididymidis. The process of spermatogenesis is associated with serval steps including spermatocytogenesis, spermatidogenesis, and spermiogenesis. Considering the underlying influence of Cd on the process of spermatogenesis, PAS-staining of the section was used to distinguish the spermatogenic tubules at different stages of the spermatogenesis process. Compared to the control group, the vast majority of spermatogonia, spermatocytes, round spermatids, and early elongating spermatids were largely stabilized in accordance with the conventional spermatogenic process for mitosis and meiosis, while condensed spermatids were strongly reduced from steps 11-12 (stages ⅩⅠ-ⅩⅡ) to the end of spermiogenesis in the seminiferous tubules of Cd group testis (Figure 3 A and 3 C). As expected, the nutritional intervention group displayed a preferable constitute of sperm cells in diverse stages of seminiferous tubules in the presence of C3G compared to the Cd group. Hence, Cd exposure in male puberty can cause defective spermatogenesis at a later spermiogeneic stage, while the C3G can restore the arrest of the spermatogenic process.

3.3 Effects of C3G on Retention of Histone-to-Protamine Exchange Caused by Cd.

Spermiogenesis is accompanied by extensive chromatin reorganization during which most of the nucleosomal histones are initially replaced by transition proteins (TNP1 and TNP2) and subsequently by protamines. Remarkably, the histone-to-protamine exchange marked with histone degradation starts from the step 11-12 of

spermiogenesis, which is highly consistent with the period of retardation found in this study. To investigate the potential causes of the spermiogenesis failure from Cd and the corresponding protective mechanisms the C3G worked on, the histone-to-protamine exchange was primarily examined. In particular, the expression of histone H2A and H2B was determined by immunohistochemically staining. There is visible retention of both kinds of histones in the elongated spermatids after damage by Cd (red arrows) which was supposed to be removed under normal circumstances, while there was no significant expression in sperms at the same steps in the presence of C3G (Figure 4 A). Accordingly, the protein expression of Histone H2A and H2B in the whole testis was upregulated in the Cd group while C3G suppressed this novel upregulation back to the level consistent with the control group (Figure 4 B-D). Subsequently, the RNA expression of Tnp1, Tnp2, Prm1, and Prm2 was downregulated in the Cd group compared to the control group, while C3G treatment predominantly reversed the expression similar to that of the conventional histone-to-protamine exchange (Figure 4 E-H). These results support the notion that C3G can rescue the Cd-induced failure of spermiogenesis by releasing the retention of histone-to-protamine exchange to allow spermatogenesis to progress.

3.4 Effects of C3G on Cd-damaged Histone Ubiquitination During Spermiogenesis.

The above mentioned histone-to-protamine exchange occurs inside of the sperm nucleus chromatin is involved in a variety of histone modification including ubiquitination, acetylation, and methylation. Firstly, we evaluated the concentration of

HDAC and HAT in the testis by ELISA and protein expression of Histone 4 (H4) together with the corresponding acetylated-H4 at different lysine sites including Lys5, Lys8, and Lys12 by western blot. Slight changes were observed in terms of HAT (Figure 5 A-B), nevertheless, no difference in the expression of H4 and acetyl-H4 between all three groups (Figure 5 C).

As another concerned item, histone ubiquitination process, the master prerequisite of nucleosome removal during sperm elongating period, was subsequently examined due to its vital role in positively degrading histones by labeling ubiquitin with ubiquitin-activating enzymes (E1), ubiquitin-conjugating enzymes (E2), and ubiquitin ligases (E3). As shown in Figure 6 A, IHC analysis demonstrated that ubiquitin histone H2A (ub-H2A) in pachytene spermatocyte was reduced, and the ubiquitin histone H2B (ub-H2B) still is present in round spermatid after Cd exposure. Interestingly, there is no abnormal distribution or expression of either ub-H2A or ub-H2B in the C3G treatment group. Multiple crucial enzymes associated with ubiquitination of H2A and H2B were profiled, and several of them were revealed as the underlying target of C3G. Administration of C3G notably upregulated the ubiquitin enzyme related to H2A ubiquitination including ring finger protein 2 (Rnf2), ring finger protein 1 (Ring 1), and DAZ interacting zinc finger protein 3 (2A-HUB) and appropriately normalized enzymes related to H2B ubiquitination such as Ring finger protein 8 (Rnf8) and Ring finger 40 (Rnf40) (Figure 6 B-C).

3.5 Effects of C3G on Cd-induced Oxidative Stress in Testis

The failure of exchange of histone-to-protamine during spermiogenesis results in the sperm nucleus not being able to be condensed and subsequently protect

themselves from exogenous oxidative damage, which may be affected by Cd exposure. Meanwhile, the unfortunate and unexpected oxidative stress induced by Cd may decide the final fate of the unaccomplished sperm. SOD can catalyze the excess superoxide radicals in the body into hydrogen peroxide. In this study, the activity of SOD was partly inhibited in the presence of Cd (Figure 7 A). GSH, an antioxidant, can prevent oxidative stress in the testis by reducing hydrogen peroxide to H_2O. After treatment of Cd, the GSH was overconsumed by Cd-produced reactive oxygen species (ROS) accompanied by a fall in the proportion of GSH/GSSG (Figure 7 B-D). As an excellent antioxidant, C3G maintained the delicate balance of the redox system by increasing the level of GSH and promoting the activity of SOD predominantly. Finally, MDA, the terminal product of lipid peroxidation, was decreased significantly with the addition of C3G to the diet (Figure 7 E).

3.6 Effects of C3G Against DNA Damage in Round Spermatids and Sperm Apoptosis.

8-OHdG is commonly considered as a biomarker of DNA damage. According to the expression of 8-OHdG in seminiferous tubule carried out by IF, on account of the Cd-mediated oxidative stress damage, the gathering of 8-OHdG in round spermatids were increased, whereas there was no DNA damage present in the C3G intervention group (Figure 7 F). Apoptotic cells from the testis section were subsequently detected by TUNEL staining. Numerous apoptotic sperm cells in the seminiferous tubule at specific stages after Cd exposure were observed, especially in primary spermatocytes and elongated spermatids (Figure 7 G). As expected, the amount of apoptotic elongated

spermatids in the C3G treatment group was declined dramatically compared to the Cd exposure group. These results figured out the positive effects of C3G prevails over the negative impact caused by Cd, allowing for sperm cells to survive DNA damage and followed apoptotic programmed death.

3.7 Effects of C3G on Expression of Proteins Involved in MAKPs Signaling Pathway.

In light of the impressionability of mitogen-activated protein kinase (MAPK) signaling pathway to oxidative stress and it is considered the master regulator of spermatogenic cell differentiation, proliferation, and apoptosis, we investigated the expression of several proteins expression involved in the MAPK signaling pathway by western blot. As shown in Figure 8 A-B, the phosphorylation of ERK and JNK was repressed after Cd exposure, and C3G notably stimulated the upregulation of them to a moderate level. Our study also elucidated that the phosphorylation level of p38, the principal MAPK protein response to oxidative stress in the testis, was improved under Cd-induced oxidative stress status, and decreased with the consumption of C3G in the diet (Figure 8 C).

3.8 Effects of C3G on Expression of Proteins Involved in Mitochondrial Apoptosis.

P53 is crucial for maintaining cell integrity and relieving various reactions under stress. The upstream pathway of p38/MAPK can phosphorylate p53 at an exclusive site unequivocally, thereby initiating the regulatory function on Bcl-2 family protein, which is involved in cell apoptosis. Cd exposure displayed the ability to increase both the level of

p53 and *p*-p53 (Figure 9 A), contributing to the rise of pro-apoptotic proteins including Bax and Bad, and the decline of anti-apoptotic proteins like Bcl-2 (Figure 9 B). Importantly, the addition of C3G protected against the aberrant expression of p53 and *p*-p53, and decreased the expression of the Bcl-2 family protein to nearly a level consistent with the control group.

The release of cytochrome C from the damaged mitochondria is under the management of disorganized Bcl-2 family protein and contributes to activation of caspase-9 and caspase-3 and giving rise to the caspase cascade. This is the pivotal and general biological marker that initiates apoptosis. As shown in Figure 9 C, Cd exposure caused caspase-3 cleavage, and supplementation of C3G partly suppressed this process. Additionally, cleaved caspase-3 has the ability to cleave the full PARP that can repair the damaged DNA double strands (Figure 9 D). Fortunately, testis from C3G treatment group exhibited a normal status of PARP that was totally different from Cd injured group, which suggested that the DNA-repairing system was intact and functioning.

Discussion

A widespread hazardous environmental contaminant derived from industries, Cd can accumulate in various organs through water, food, and air, and trigger male reproductive damage, which is correlated with male infertility and poor semen quality [6,7]. Although this issue has received extraordinary attention, current research rarely investigates the reproductive toxicity of Cd in puberty or whether the nutritional intervention can be a feasible solution [24,25]. Anthocyanin is a well-known water-soluble and bioactive

phytochemical frequently found in fruits, vegetables, and grains, which can possibly provide an increasingly important strategy in the prevention of several diseases [19]. In our previous study, C3G, a prevalent anthocyanin has been shown to have an ability to reverse Cd-induced dysfunction of sex hormone regulation in *vitro* and *in vivo* [18,21]. However, the damage on spermatogenesis from Cd in puberty and the relevant protective effect from C3G still remains unclear. Thus drawing from the experience from our previous studies, C3G at the dose of 500 mg/kg in the diet that in accordance with the actual consumption of human daily intake was efficiently used for exploring the effect and underlying mechanisms of C3G against Cd-induced spermatogenesis dysfunction.

In mammals, the blood-testis-barrier, which divides the seminiferous epithelium into basement membrane and adluminal compartment, is generally elucidated as one of the paramount targets of Cd toxicity in testes. The BTB is composed of tight junction, adherens junction, and gap junctions by Sertoli cell and can provide an immunologic barrier and confer a germ cell-friendly microenvironment for spermatogenesis [26,27]. Failure of spermatogenesis is unequivocally coupled with the destruction of the BTB when exposed to Cd at sexual maturity *via* intraperitoneal injection [10]. Intriguingly, there was no obvious structural damage or BTB collapse found in seminiferous epithelium using oral ingestion in puberty in this study. This finding is consistent with the previous studies involving Cd reproductive toxicity at puberty or sexual maturity *via* the oral route [25,28,29]. Thus, the damage from Cd on the mice male reproductive system may highly depend on the methods of administration and represent an age-dependent effect.

Remarkably, reduction in average testis weight and sperm counts, as well as fewer movement and forward progression of sperms were observed in the Cd exposure mice, while supplementation of C3G successfully attenuated these effects. To understand the specific underlying mechanism, we examined the stages of seminiferous epithelium cycles by PAS staining, which indicated that spermatogenesis was blocked from step 11-12 (stage ⅪⅠ-ⅫⅠ) during spermiogenesis with a largely reduced number of condensed spermatids in the seminiferous tubules of Cd exposed mice and this was recovered in the presence of C3G treatment. Spermiogenesis that is accompanied by the whole indispensable transformation from haploid spermatids after meiosis to mature elongated spermatids was subdivided into 16 steps involved in the distinctive and unique feature of histone-to-protamine exchange in sperm head for chromatin recombination that uniformly occurred at steps 11-12. This change defined a gradual replacement of histone to transition proteins and subsequent protamines allow for a highly condensed DNA-protamine complex generation in sperm nucleus which packages the genomic DNA into tiny sperm heads and sets the integrated DNA at a stable and non-transcriptional state with the characteristic of sperm flexibility strengthen and oxidative stress prevention. We further asked whether there is a defect in the presentation of histone, transition protein, and protamine. Excitingly, Cd exposure during puberty negatively interfered with the histone-to-protamine exchange as seen by severe histone retention and unconventionally lower gene expression of transition protein and protamine. As expected, C3G treatment mitigated this damage replacement process and restored normal spermatogenesis.

Epigenetic toxicity derived from Cd-caused oxidative stress is closely associated

with the progression of multifarious diseases by aberrant DNA methylation and histone modification [16,30,31]. Regular acetylation and ubiquitination are crucial parts of histone modification as well as play a prerequisite role on the histone-to-protamine exchange [14,32,33]. Hyperacetylation of histones catalyzed by HAT and HDAC at different lysine residual sites is essential to the degradation of core histones [32,34], which also can be demonstrated as the target of Cd in male puberty *via* intraperitoneal injection [17]. However, in the present study *via* oral exposure, the unaltered protein expression of acetylated histone H4 in all groups indicated that the damage from Cd and protective effects from C3G were not related to histone acetylation. Next, the alteration of ubiquitination was considered. As the initial step in histone-to-protamine exchange, histone ubiquitination can facilitate histone removal by loosening the compact nucleosome [14], subsequently, promoting the replacement of transition protein in pachytene spermatocyte [35]. Within this pivotal course, several affected critical enzymes associated with histone H2A ubiquitination including Rnf2, Ring1, Bmi, 2A-HUB and histone H2B and ubiquitination including Rnf8 and Rnf40 were examined respectively. Notably, C3G treatment partly regulated expression of some of the enzymes such as Rnf2, Ring1, 2A-HUB, and Rnf8 and properly normalized histone ubiquitination, which prompted successful histone-to-protamine exchange. However, studies looking into the specific regulatory mechanisms of C3G on ubiquitin enzyme is warranted.

Failure of histone-to-protamine exchange disastrously resulted in an exposed and unprotected sperm nucleus that is easily vulnerable to oxidative stress [36]. Given that Cd overexposure can lead to an overconsumption of anti-oxidase by ROS accumulation

[37] as well as directly cause destruction of antioxidant system by devitalizing anti-oxidase such as GSH [38], Cd generated oxidative damage would give a second deeper strike to the unaccomplished sperms. Primarily, anthocyanin as a bioactive compound with the property of effectively scavenging free radicals and terminating chain reaction of oxidative damage, has been shown to protect against oxidative stress in multiple organs including testis [39,40]. Consumption of C3G in this study played a critical role in balancing the antioxidative system by increasing GSH levels and promoting the activity of SOD in testis. Therefore, the overproduced $O_2^{-\cdot}$ could be catalyzed into H_2O_2 by SOD and eventually to H_2O and O_2 by GSH, which protected the testis from Cd-induced oxidative stress. Additionally, there was significant DNA damage found in haploid sperm after Cd exposure. More importantly, histones can migrate from the nucleus into the cytoplasm as a response of DNA double-strand breakage and then can indirectly activate BAK at the mitochondrial outer membrane, resulting in the promotion of cytochrome C release and activation of a cell programmed apoptosis [41]. Additionally, taking together with the impaired DNA-caused p53 disinhibition [42] and oxidative stress-induced upstream JNK/MAPK and p38/MAPK phosphorylation [43], p53 were active and transported towards cytoplasm, and accordingly interacted with anti-apoptotic proteins Bcl-2 and Bcl-xL or activated Bax, forming a mitochondrial transition pore [44,45]. Finally, cytochrome C was released through this permeable pore and the corresponding apoptosis cellular signal transduction is activated, which give rise to cell apoptosis. Consequently, in this study, C3G mitigated the DNA damage, which we believe is attributed to its remarkable antioxidative ability. Simultaneously, C3G appropriately regulated the MAPK signaling pathway for the requisite inhibition of p53 to

avoid the occurrence of sperm cell apoptosis.

Conclusion

In conclusion, Cd exerts reproductive toxicity on the testis. It also has been demonstrated that the concentration of Cd in the blood and semen is inversely correlated to semen quality, which indicates that Cd exposure plays an extremely hazardous role in male infertility. Recently, flavonoids with strong bioactivity including anthocyanin have been considered a potential antagonist to Cd toxicity. However, studies examing the effect of Cd on spermatogenesis and dietary intervention during puberty is still lacking. In the present study, Cd exposure caused an obvious reduction in total number, viability, and progressive motility of sperms in male pubertal mice. Interestingly the prevalent anthocyanin C3G effectively protects spermatogenesis in male pubertal mice from the damage elicited by Cd *via* normalizing histone modification, restoring the histone to protamine exchanges in spermiogenesis, and improving the anti-oxidative system in the testis, subsequently alleviating apoptosis. Taken altogether, the results of this study suggest that consumption of anthocyanins can be protective against Cd-induced male pubertal reproductive dysfunction. Further investigation to examine the dose-dependent effects and also the effect on humans should be conducted in the future.

CRediT author statement

Xusheng Li: Methodology, Investigation, Formal analysis, Writing-Original Draft

Zilan Yao: Writing-Original Draft

Dacheng Yang: Validation, Data Curation

Xinwei Jiang: Methodology

Jianxia Sun: Visualization

Lingmin Tian: Resources

Biyu Wu: Writing-Review & Editing

Weibin Bai: Conceptualization, Supervision, Project administration

Conflict of interest

The authors declare no competing financial interest.

Acknowledgments

This work was supported by Guangdong Key Area Research and Development Program (NO. 2019B02021003). The authors also thank the Science and Technology Program of Guangzhou (NO. 201903010082 and NO. 201704020050) and National Natural Science Foundation of China (NO. 81703211). Dr. Jazmyne from Prof. Hennig' s lab (University of Kentucky) was appreciated for providing editorial assistance. We gratefully acknowledge the work of Dr. Shun Bai and Dr. Jiao Luo for providing the suggestion of experiments. We also acknowledge Junliang Chen, Xia Li, Jingting Guo, Xinyu Ni, Ziyao Peng, Guowei Chen, and Lei Zhang for assistance with the animal work and tissue collection.

Reference

[1] H. Levine, N. Jorgensen, A. Martino-Andrade, J. Mendiola, D. Weksler-Derri, I. Mindlis, R. Pinotti, S.H. Swan, Temporal trends in sperm count: A systematic review and meta-regression analysis, Human Reproduction Update. 23 (2017) 646-659.

[2] E.W. Wong, C.Y. Cheng, Impacts of environmental toxicants on male reproductive dysfunction, Trends in Pharmacological Sciences. 32 (2011) 290-299.

[3] C.Y. Wu, C.S. Wong, C.J. Chung, M.Y. Wu, Y.L. Huang, P.L. Ao, Y.F. Lin, Y.C. Lin, H.S. Shiue, C.T. Su, H.H. Chen, Y.M. Hsueh, The association between plasma selenium and chronic kidney disease related to lead, cadmium and arsenic exposure in a Taiwanese population, Journal of Hazardous Materials. 375 (2019) 224-232.

[4] J. Thompson, J. Bannigan, Cadmium: Toxic effects on the reproductive system and the embryo, Reproductive Toxicology. 25 (2008) 304-315.

[5] T.Y. Zhong, D.W. Xue, L.M. Zhao, X.Y. Zhang, Concentration of heavy metals in vegetables and potential health risk assessment in China, Environmental Geochemistry and Health. 40 (2018) 313-322.

[6] W. Guzikowski, M.I. Szynkowska, H. Motak-Pochrzest, A. Pawlaczyk, S. Sypniewski, Trace elements in seminal plasma of men from infertile couples, Archives of Medical Science. 11 (2015) 591-598.

[7] J. Mendiola, J.M. Moreno, M. Roca, N. Vergara-Juarez, M.J. Martinez-Garcia, A. Garcia-Sanchez, B. Elvira-Rendueles, S. Moreno-Grau, J.J. Lopez-Espin, J. Ten, R. Bernabeu, A.M. Torres-Cantero, Relationships between heavy metal

concentrations in three different body fluids and male reproductive parameters: a pilot study, Environmental Health. 10 (2011) 7.

[8] N. Pant, G. Upadhyay, S. Pandey, N. Mathur, D.K. Saxena, S.P. Srivastava, Lead and cadmium concentration in the seminal plasma of men in the general population: correlation with sperm quality, Reproductive Toxicology. 17 (2003) 447-450.

[9] C. de Angelis, M. Galdiero, C. Pivonello, C. Salzano, D. Gianfrilli, P. Piscitelli, A. Lenzi, A. Colao, R. Pivonello, The environment and male reproduction: The effect of cadmium exposure on reproductive function and its implication in fertility, Reproductive Toxicology. 73 (2017) 105-127.

[10] H.L. Dong, Z.G. Chen, C.X. Wang, Z. Xiong, W.L. Zhao, C.H. Jia, J. Lin, Y. Lin, W.P. Yuan, A.Z. Zhao, X.C. Bai, Rictor regulates spermatogenesis by controlling sertoli cell cytoskeletal organization and cell polarity in the mouse testis, Endocrinology. 156 (2015) 4244-4256.

[11] N. Babaknejad, S. Bahrami, A.A. Moshtaghie, H. Nayeri, P. Rajabi, F.G. Iranpour, Cadmium testicular toxicity in male wistar rats: Protective roles of zinc and magnesium, Biological Trace Element Research. 185 (2018) 106-115.

[12] R.S. Almeer, D. Soliman, R.B. Kassab, G.I. AlBasher, S. Alarifi, S. Alkahtani, D. Ali, D. Metwally, A.E.A. Moneim, Royal Jelly abrogates cadmium-induced oxidative challenge in mouse testes: Involvement of the Nrf2 pathway, International Journal of Molecular Sciences. 19 (2018) 17.

[13] E.R. Siu, D.D. Mruk, C.S. Porto, C.Y. Cheng, Cadmium-induced testicular injury, Toxicology and Applied Pharmacology. 238 (2009) 240-249.

[14] L.T. Gou, J.Y. Kang, P. Dai, X. Wang, F. Li, S. Zhao, M. Zhang, M.M. Hua, Y. Lu, Y. Zhu, Z. Li, H. Chen, L.G. Wu, D.S. Li, X.D. Fu, J.S. Li, H.J. Shi, M.F. Liu, Ubiquitination-deficient mutations in human piwi cause male infertility by impairing Histone-to-Protamine exchange during spermiogenesis, Cell. 169 (2017) 1090-1104.

[15] B. Suresh, J. Lee, S.H. Hong, K.S. Kim, S. Ramakrishna, The role of deubiquitinating enzymes in spermatogenesis, Cellular and Molecular Life Sciences. 72 (2015) 4711-4720.

[16] M. Li, C. Liu, L.L. Yang, L. Zhang, C.H. Chen, M.D. He, Y.H. Lu, W. Feng, H.F. Pi, Y.W. Zhang, M. Zhong, Z.P. Yu, Z. Zhou, G9a-mediated histone methylation regulates cadmium-induced male fertility damage in pubertal mice, Toxicology Letters. 252 (2016) 11-21.

[17] Q.Z. Yang, P.F. Li, Y. Wen, S.S. Li, J. Chen, X.R. Liu, L.R. Wang, X.H. Li, Cadmium inhibits lysine acetylation and succinylation inducing testicular injury of mouse during development, Toxicology Letters. 291 (2018) 112-120.

[18] X.S. Li, J.T. Guo, X.W. Jiang, J.X. Sun, L.M. Tian, R. Jiao, Y.G. Tang, W.B. Bai, Cyanidin-3-O-glucoside protects against cadmium-induced dysfunction of sex hormone secretion via the regulation of hypothalamus-pituitary-gonadal axis in male pubertal mice, Food and Chemical Toxicology. 129 (2019) 13-21.

[19] X.W. Jiang, X.S. Li, C.J. Zhu, J.X. Sun, L.M. Tian, W. Chen, W.B. Bai, The target cells of anthocyanins in metabolic syndrome, Critical Reviews in Food Science & Nutrition. (2018) 1-71.

[20] X. Li, X.W. Jiang, J.X. Sun, C.J. Zhu, X.L. Li, L.M. Tian, L. Liu, W.B. Bai,

Cytoprotective effects of dietary flavonoids against cadmium-induced toxicity, Annals of the New York Academy of Sciences. 1398 (2017) 5-19.

[21] X. Li, J.L. Lu, J.X. Sun, X.W. Jiang, X.S. Li, Y. Li, R. Jiao, L.M. Tian, W.B. Bai, Cyanidin-3-O-glucoside promotes progesterone secretion by improving cells viability and mitochondrial function in cadmium-sulfate-damaged R2C cells, Food and Chemical Toxicology. 128 (2019) 97-105.

[22] X.W. Jiang, C.J. Zhu, X.S. Li, J.X. Sun, L.M. Tian, W.B. Bai, Cyanidin-3-O-glucoside at low doses protected against 3-chloro-1,2-propanediol induced testis injury and improved spermatogenesis in male rats, Journal of Agricultural and Food Chemistry. 66 (2018) 12675-12684.

[23] F. Erdemir, D. Atilgan, F. Markoc, O. Boztepe, B. Suha-Parlaktas, S. Sahin, The effect of diet induced obesity on testicular tissue and serum oxidative stress parameters, Actas Urologicas Espanolas. 36 (2012) 153-159.

[24] M. Interdonato, G. Pizzino, A. Bitto, F. Galfo, N. Irrera, A. Mecchio, G. Pallio, V. Ramistella, F. De Luca, A. Santamaria, L. Minutoli, H. Marini, F. Squadrito, D. Altavilla, Cadmium delays puberty onset and testis growth in adolescents, Clinical Endocrinology. 83 (2015) 357-362.

[25] Y.L. Ji, H. Wang, P. Liu, Q. Wang, X.F. Zhao, X.H. Meng, T. Yu, H. Zhang, C. Zhang, Y. Zhang, D.X. Xu, Pubertal cadmium exposure impairs testicular development and spermatogenesis via disrupting testicular testosterone synthesis in adult mice, Reproductive Toxicology. 29 (2010) 176-183.

[26] P. Mital, B.T. Hinton, J.M. Dufour, The blood-testis and blood-epididymis barriers are more than just their tight junctions, Biology of Reproduction. 84 (2011) 851-

858.

[27] M.P. Hedger, Immunophysiology and pathology of inflammation in the testis and epididymis, Journal of Andrology. 32 (2011) 625-640.

[28] A. Blanco, R. Moyano, J. Vivo, R. Flores-Acuna, A. Molina, C. Blanco, E. Aguera, J.G. Monterde, Quantitative changes in the testicular structure in mice exposed to low doses of cadmium, Environmental Toxicology and Pharmacology. 23 (2007) 96-101.

[29] M.F. Medina, M.C. Arrieta, M.N. Villafane, S.M.R. Klyver, I.M.A. Odstrcil, M.E. Gonzalez, Early signs of toxicity in testes and sperm of rats exposed to low cadmium doses, Toxicology and Industrial Health. 33 (2017) 576-587.

[30] M. Takiguchi, W.E. Achanzar, W. Qu, G.Y. Li, M.P. Waalkes, Effects of cadmium on DNA-(Cytosine-5) methyltransferase activity and DNA methylation status during cadmium-induced cellular transformation, Experimental Cell Research. 286 (2003) 355-365.

[31] L. Benbrahim-Tallaa, R.A. Waterlandz, A.L. Dill, M.M. Webber, M.P. Waalkes, Tumor suppressor gene inactivation during cadmium-induced malignant transformation of human prostate cells correlates with overexprression of de Novo DNA methyltransferase, Environmental Health Perspectives. 115 (2007) 1454-1459.

[32] M.X. Qian, Y. Pang, C.H. Liu, K. Haratake, B.Y. Du, D.Y. Ji, G.F. Wang, Q.Q. Zhu, W. Song, Y.D. Yu, X.X. Zhang, H.T. Huang, S.Y. Miao, L.B. Chen, Z.H. Zhang, Y.N. Liang, S. Liu, H.H. Cha, D. Yang, Y.G. Zhai, T. Komatsu, F. Tsuruta, H.T. Li, C. Cao, W. Li, G.H. Li, Y.F. Cheng, T. Chiba, L.F. Wang, A.L. Goldberg, Y. Shen,

X.B. Qiu, Acetylation-mediated proteasomal degradation of core histones during DNA repair and spermatogenesis, Cell. 153 (2013) 1012-1024.

[33] B. Fierz, C. Chatterjee, R.K. McGinty, M. Bar-Dagan, D.P. Raleigh, T.W. Muir, Histone H2B ubiquitylation disrupts local and higher-order chromatin compaction, Nature Chemical Biology. 7 (2011) 113-119.

[34] J. Govin, E. Escoffier, S. Rousseaux, L. Kuhn, M. Ferro, J. Thevenon, R. Catena, I. Davidson, J. Garin, S. Khochbin, C. Caron, Pericentric heterochromatin reprogramming by new histone variants during mouse spermiogenesis, Journal of Cell Biology. 176 (2007) 283-294.

[35] W.M. Baarends, J.W. Hoogerbrugge, H.P. Roest, M. Ooms, J. Vreeburg, J.H. Hoeijmakers, J.A. Grootegoed, Histone ubiquitination and chromatin remodeling in mouse spermatogenesis, Developmental biology. 207 (1999) 322-333.

[36] C.C. Boissonnas, P. Jouannet, H. Jammes, Epigenetic disorders and male subfertility, Fertility and Sterility. 99 (2013) 624-631.

[37] T.L. Bu, Y.L. Mi, W.D. Zeng, C.Q. Zhang, Protective effect of quercetin on cadmium-induced oxidative toxicity on germ cells in male mice, Anatomical Record-Advances in Integrative Anatomy and Evolutionary Biology. 294 (2011) 520-526.

[38] K. Jomova, M. Valko, Advances in metal-induced oxidative stress and human disease, Toxicology. 283 (2011) 65-87.

[39] A. Zepeda, L.G. Aguayo, J. Fuentealba, C. Figueroa, A. Acevedo, P. Salgado, G.M. Calaf, J. Farias, Blueberry extracts protect testis from hypobaric hypoxia induced oxidative stress in rats, Oxidative Medicine and Cellular Longevity. (2012) 7.

[40] H. Jang, S.J. Kim, S.M. Yuk, D.S. Han, U.S. Ha, S.H. Hong, J.Y. Lee, T.K. Hwang,

S.Y. Hwang, S.W. Kim, Effects of anthocyanin extracted from black soybean seed coat on spermatogenesis in a rat varicocele-induced model, Reproduction Fertility and Development. 24 (2012) 649-655.

[41] A. Konishi, S. Shimizu, J. Hirota, T. Takao, Y.H. Fan, Y. Matsuoka, L.L. Zhang, Y. Yoneda, Y. Fujii, A.I. Skouitchi, Y. Tsujimoto, Involvement of histone H1.2 in apoptosis induced by DNA double-strand breaks, Cell. 114 (2003) 673-688.

[42] L.T. Vassilev, B.T. Vu, B. Graves, D. Carvajal, F. Podlaski, Z. Filipovic, N. Kong, U. Kammlott, C. Lukacs, C. Klein, N. Fotouhi, E.A. Liu, In vivo activation of the p53 pathway by small-molecule antagonists of MDM2, Science. 303 (2004) 844-848.

[43] P. Bragado, A. Armesilla, A. Silva, A. Porras, Apoptosis by cisplatin requires p53 mediated p38 alpha MAPK activation through ROS generation, Apoptosis. 12 (2007) 1733-1742.

[44] M. Mihara, S. Erster, A. Zaika, O. Petrenko, T. Chittenden, P. Pancoska, U.M. Moll, p53 has a direct apoptogenic role at the mitochondria, Molecular Cell. 11 (2003) 577-590.

[45] J.E. Chipuk, T. Kuwana, L. Bouchier-Hayes, N.M. Droin, D. Newmeyer, M. Schuler, D.R. Green, Direct activation of Bax by p53 mediates mitochondrial membrane permeabilization and apoptosis, Science. 303 (2004) 1010-1014.

Table 1 Primer sequence for qPCR in this study.

Gene name	Accession No.	Primer sequence (5'→3')	
Tnp1	NM_009407	Forward	ACCAGCCGCAAGCTAAAGAC
		Reverse	GCTTCCACCTCTCTTGACGC
Tnp2	NM_013694	Forward	GCTCAGGGCGAAGATACAAGTG
		Reverse	TGTGACATCATCCCAACAGTCC
Prm1	NM_013637	Forward	CCGTCGCAGACGAAGATGTC
		Reverse	CACCTTATGGTGTATGAGCGG
Prm2	NM_008933	Forward	GTAGGAGGCACCATCACTAAGC
		Reverse	AGACATCGACATGGAATGGTG
Rnf2	NM_011277	Forward	AACACCTCAGGAGGCAATAACA
		Reverse	GCGCAAAACCGATGTAAACACT
Ring1	NM_009066	Forward	GGAGTGCCTGCATAGGTTCTG
		Reverse	TAGGGACCGCTTGGATACCA
Bmi1	NM_007552	Forward	ACGTCATGTATGAAGAGGAACCT
		Reverse	TGGCCGAACTCTGTATTTCAAAG
2A-HUB	NM_027341	Forward	GAAAGAGGACTGCATAGAAGCTG
		Reverse	TCGAAGTAAACCACGTCCAAAA
Ube2d3	NM_025356	Forward	GAAAGAGGACTGCATAGAAGCTG
		Reverse	GGGCTGTCATTAGGTCCCATAA
Brca1	NM_009764	Forward	AGGAGGCGTCGATCATCCA
		Reverse	ACAGATTTCTTTCGAGGTTGGG
Ube2a	NM_019668	Forward	GGGACTTCAAGAGGTTACAGGA
		Reverse	TCTGCATAGACGTTAGGATGGA
Ube2b	NM_009458	Forward	AAATAAACCACCAACCGTTAGGT
		Reverse	TCTCTTCTCATACTCCCGTTTGT
Rnf8	NM_021419	Forward	GACCATAGGACGGGGACTTAG
		Reverse	GTTCAGCCAAACACCATTCAGA
Rnf20	NM_182999	Forward	AGCAGAAATGCTAGATCAGCG
		Reverse	GCGGATGTTTTCATCAAACTGG
Rnf40	NM_172281	Forward	AAGACCACGACCACTCTAATCG
		Reverse	TCCAATTTCTCAATTCTCTCCCG
Gapdh	NM_008084	Forward	AATGGATTTGGACGCATTGGT
		Reverse	TTTGCACTGGTACGTGTTGAT

Table 2 Changes in anogenital distance, testis and epididymis weight and relative weight.

Groups		Control	Cd	Cd+C3G
Anogenital Distance/cm	0 d	1.33±0.06^{a}	1.30±0.10^{a}	1.37±0.07^{a}
	10 d	1.44±0.11^{a}	1.43±0.14^{a}	1.46±0.07^{a}
	20 d	1.47±0.10^{a}	1.46±0.07^{a}	1.50±0.11^{a}
	30 d	1.76±0.19^{a}	1.51±0.21^{b}	1.64±0.15^{ab}
Testis weight/mg	0 d	35.41±2.62^{a}	33.10±7.99^{a}	32.06±4.14^{a}
	10 d	72.59±9.47^{ab}	80.6±7.10^{a}	67.50±11.56^{b}
	20 d	98.63±15.16^{a}	92.35±13.16^{a}	93.45±14.27^{a}
	30 d	113.50±18.64^{a}	94.30±17.63^{b}	119.03±10.74^{a}
Testis index/%	0 d	0.47±0.06^{a}	0.46±0.50^{a}	0.49±0.50^{a}
	10 d	0.50±0.09^{a}	0.55±0.50^{a}	0.51±0.10^{a}
	20 d	0.56±0.08^{a}	0.60±0.12^{a}	0.56±0.10^{a}
	30 d	0.56±0.08^{b}	0.60±0.12^{ab}	0.66±0.10^{a}
Epididymis weight/mg	0 d	7.93±1.34^{a}	8.08±0.88^{a}	7.80±2.17^{a}
	10 d	17.43±2.04^{a}	16.46±2.21^{a}	18.78±5.16^{a}
	20 d	27.24±3.14^{a}	25.40±5.85^{a}	26.07±4.26^{a}
	30 d	36.11±3.57^{a}	34.49±7.19^{a}	35.28±3.24^{a}
Epididymis index/%	0 d	0.57±0.12^{a}	0.60±0.08^{a}	0.55±0.13^{a}
	10 d	1.24±0.15^{a}	1.12±0.12^{a}	1.41±0.31^{a}
	20 d	1.52±0.19^{a}	1.60±0.42^{a}	1.52±0.23^{a}
	30 d	1.78±0.17^{a}	1.94±0.40^{a}	1.94±0.21^{a}

*Comparison between all groups were evaluated through One-way ANOVA. Data were shown as mean±SD. Day 0, n=4; day 10 & 20, n=8; day 30, n≥9. Different letters indicate a significant difference between the groups at the equal treating time point

Table 3 Sperm motility parameter of mice treated for 30 days..

Parameters	Control	Cd	Cd+C3G
VSL/(μm/s)	27.90±9.63[a]	13.04±7.16[b]	23.79±6.12[a]
VCL/(μm/s)	29.88±10.09[a]	13.84±7.55[b]	25.44±6.41[a]
VAP/(μm/s)	20.98±7.09[a]	9.72±5.30[b]	17.86±4.50[a]
VLH/(μm)	8.90±3.01[a]	4.13±2.25[b]	7.58±1.91[a]
BCF/(Hz)	2.44±1.10[a]	1.10±0.73[b]	2.33±0.92[a]
LIN	0.93±0.01[a]	0.94±0.02[a]	0.93±0.01[a]
MAD	2.62±1.17[a]	1.18±0.79[b]	2.49±0.98[a]
STR	1.33±0.01[a]	1.34±0.03[a]	1.33±0.01[a]

*VSL, Straight-line velocity; VCL, Curvilinear velocity; VAP, Average path velocity; VLH, Amplitude of lateral head displacement; BCF, Beat-cross frequency; MAD, Mean angular displacement; LIN, Linearity; STR, Straightness coefficient.
*Comparison between all groups were evaluated through the Kruskal-Wallis Test. Data were shown as mean±SD. n≥9 (except for LIN and STR, n≥8, due to the unavailable data in one mouse without moving sperm in Cd group). Different letters indicate a significant difference between the groups at the equal treating time point.

Figure 1 Sperm counts and activity.

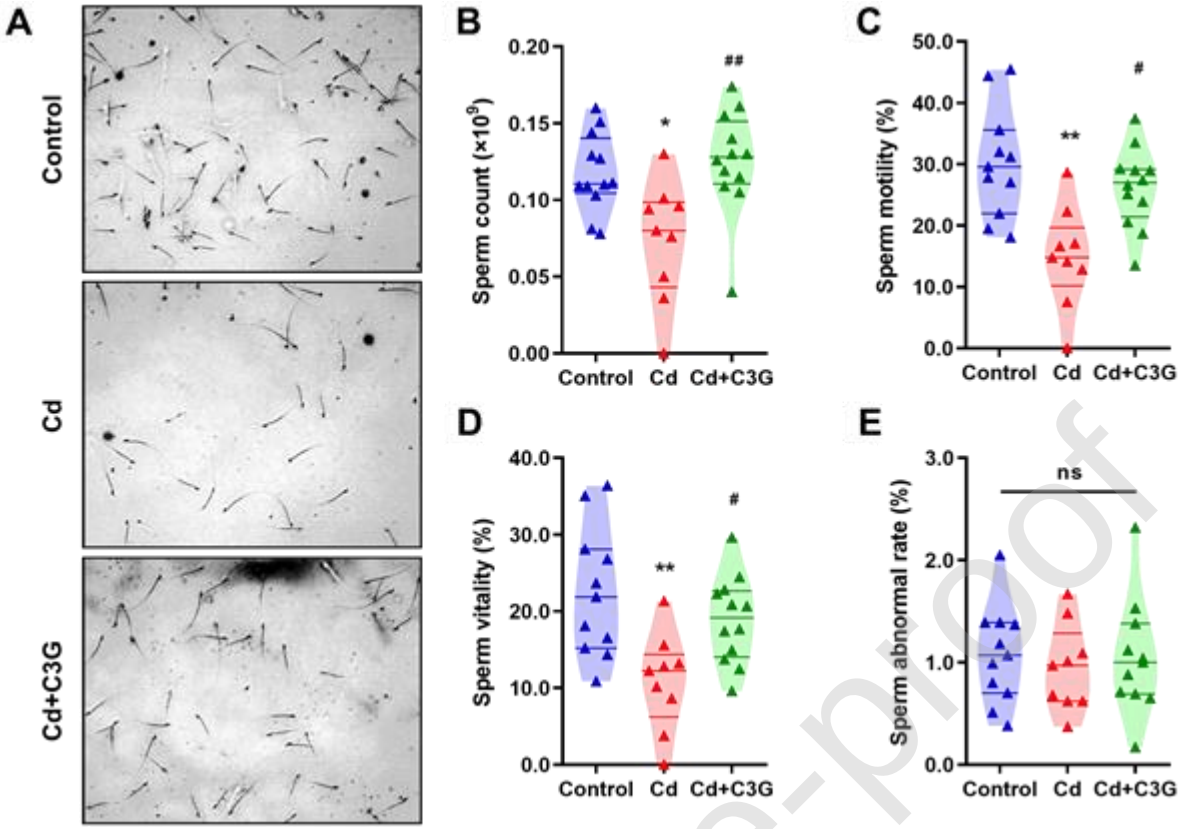

The cauda epididymal sperms from mice treated for 30 d were obtained for sperm morphology analysis, sperm counts, motility, vitality and abnormal rate by CASA. (A) Sperm captures. (B) Sperm counts. (C) Sperm motility. (D) Sperm vitality. Comparison between all groups was evaluated through the Kruskal-Wallis Test. Median with range. n≥9. $^{**}p<0.01$, $^{*}p<0.05$, compared with control group. $^{\#\#}p<0.01$, $^{\#}p<0.05$, compared with Cd group. ns, not significant.

Figure 2 The representative H&E staining histopathology of testis and epididymis.

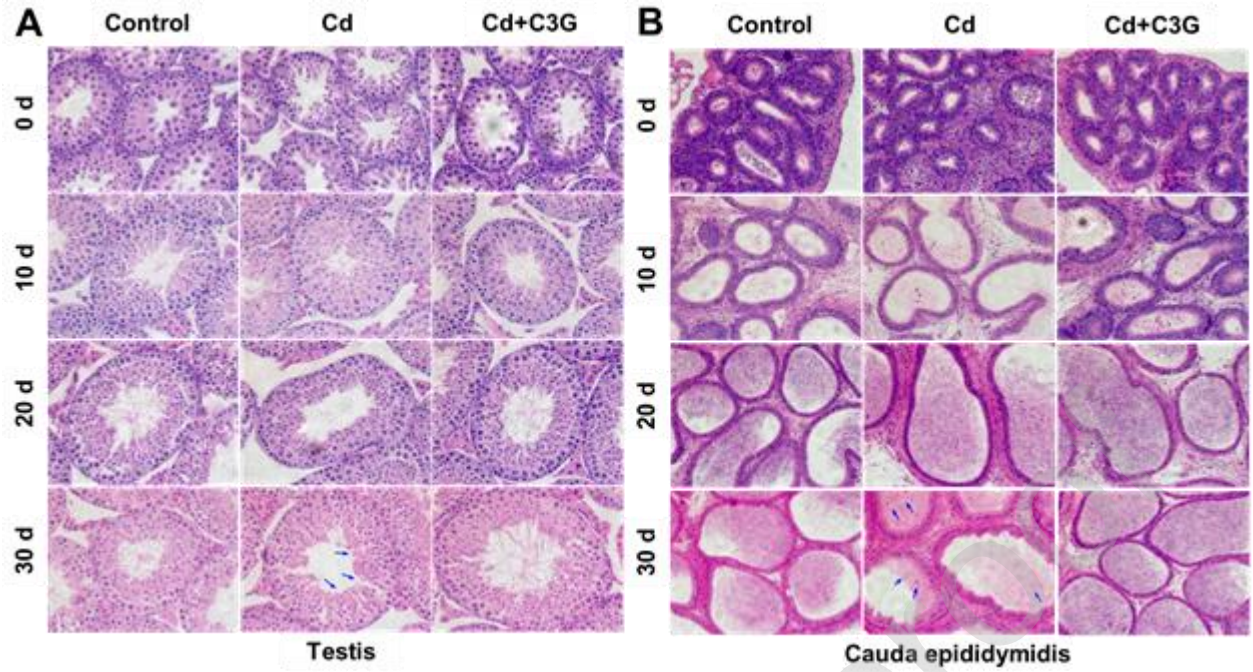

The testis and epididymis were collected embedded, cut into 5 μm slides for H&E staining and histological analysis. (A) The structure of spermatogenic tubule in testis. The blue arrow presents the lower count of elongated sperms in the lumen of the spermatogenic tubule. (B) The cauda epididymis. The blue arrow points the lower density of sperms.

Figure 3 Analysis of seminiferous epithelium and the determination of spermiogenesis.

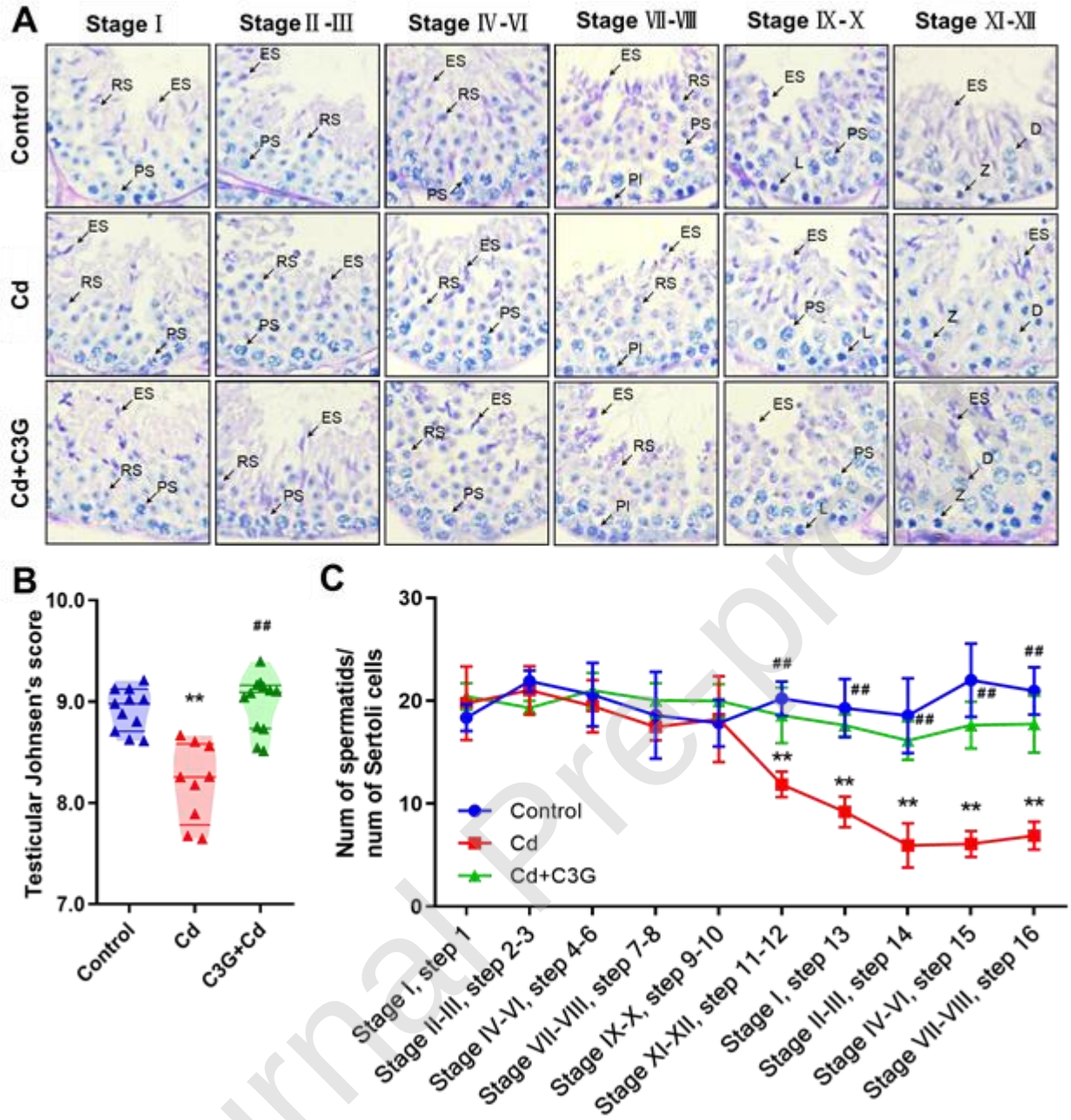

(A) Stages of seminiferous epithelium cycles determined by PAS staining. PAS staining of testis sections from mice treated for 30 days. Stages of seminiferous epithelium cycles were determined by the morphology of spermatocytes and round spermatids. RS, Round spermatid; ES, Elongated spermatid; PS, Pachytene spermatocyte; PI, Preleptotene; L, Leptotene; Z, Zygotene; D, Diplotene. (B) Testicular Johnsen's score of mice treated for 30 days. The seminiferous epithelium was evaluated according to the description of Johnsen's score standard. Comparison between all groups was evaluated

through the Kruskal-Wallis Test. Median with range. n≥9. **p<0.01, compared with control group. $^{\#\#}p$<0.01, compared with Cd group. (C) Ratios between spermatids and Sertoli cells at different steps. Ratios between spermatids and Sertoli cells in tubule cross-sections of specific stages of seminiferous epithelial cycles and corresponding spermatid development steps were shown. Comparison between all groups was evaluated through One-way ANOVA. Mean±SD. n=6. **p<0.01, compared with control group. $^{\#\#}p$<0.01, compared with Cd group.

Figure 4 The observation of histone-to-protamine exchange.

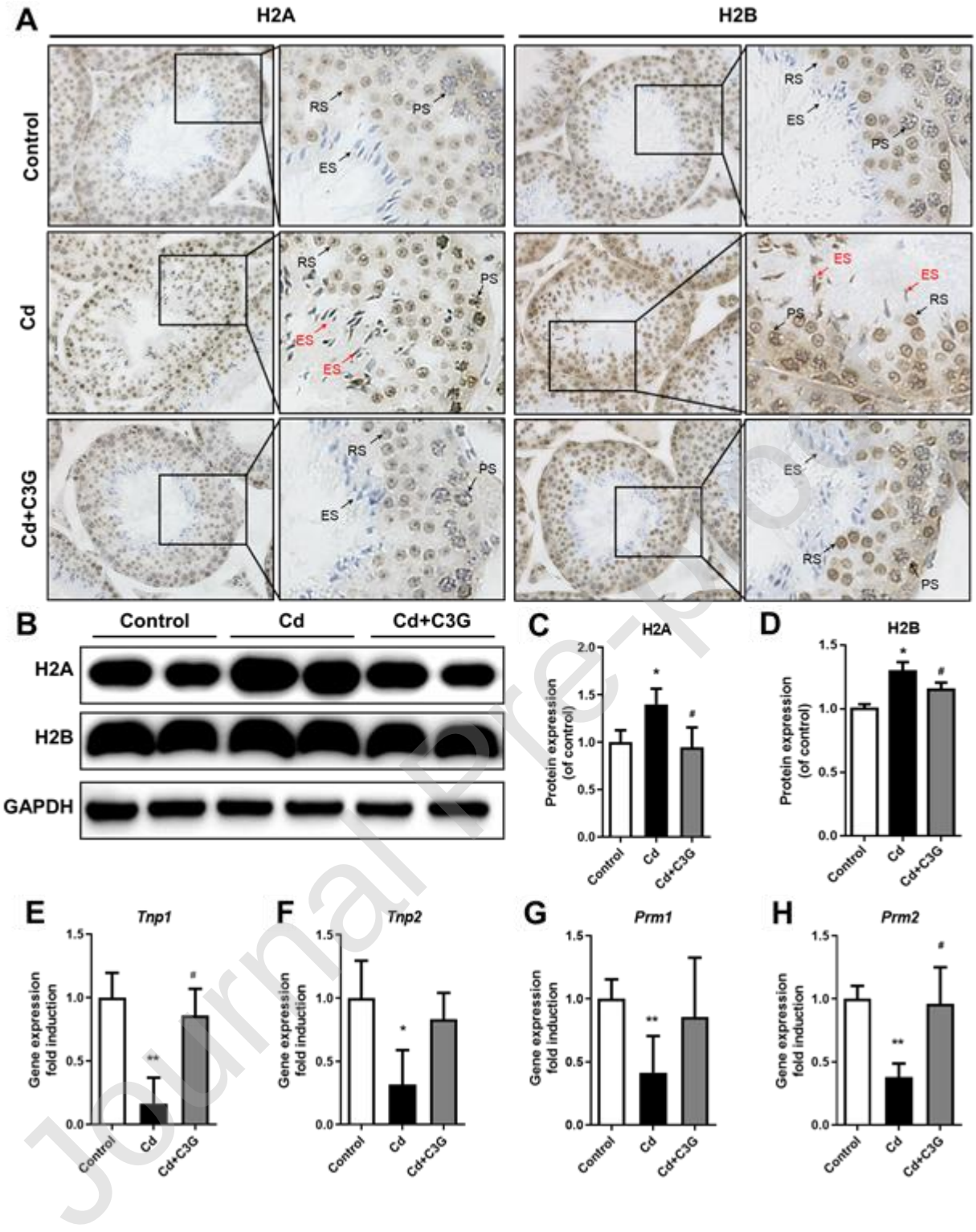

(A) The immunohistochemical analysis of Histone H2A and H2B in the seminiferous tubule at stage Ⅶ-Ⅷ from mice treated for 30 days. RS, Round spermatid; ES, Elongated spermatid; PS, Pachytene spermatocyte; PI, Preleptotene. (B-D) The representative photographs of proteins involved in Histone H2A and H2B from Western

Blots and grayscale analysis. (E-H) The mRNA expression level of transition protein and protamine in testis. Comparison between all groups was evaluated through One-way ANOVA. Mean±SD. n=4. $^{**}p<0.01$, $^{*}p<0.05$, compared with control group. $^{\#\#}p<0.05$, $^{\#}p<0.05$, compared with Cd group.

Figure 5 The determination of histone acetylation.

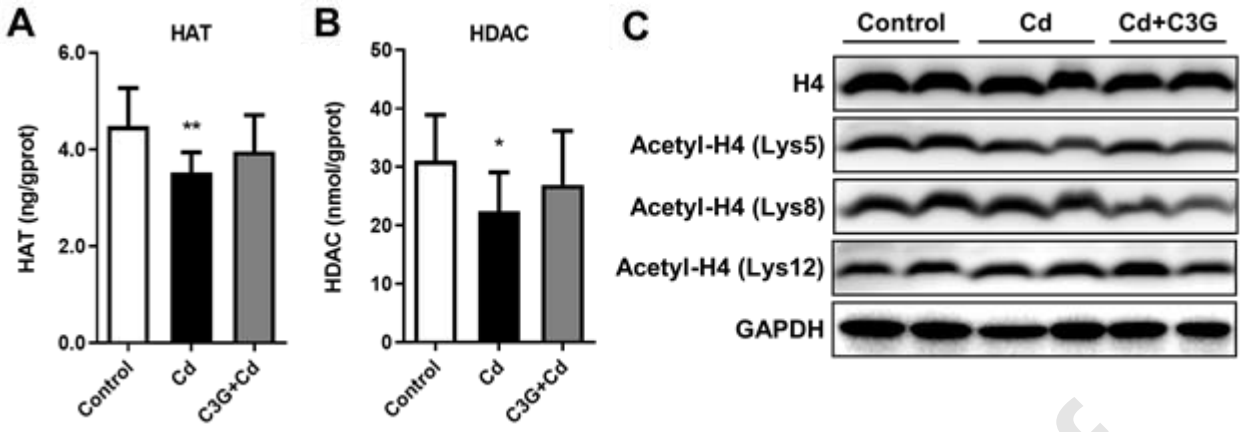

(A-B) The level of histone deacetylase (HDAC) and histone acetyltransferase (HAT) in testis from mice treated for 30 days were measured by ELISA kits. Comparison between all groups was evaluated through One-way ANOVA. Mean±SD. n≥9. *p<0.05, compared with control group. ns, not significant. (C) The protein expression level of Histone H4 and acetylated H4 at different sites in testis**.** The representative photographs of proteins involved in Histone H4, acetyl-H4 (Lys5), acetyl-H4 (Lys8), and acetyl-H4 (Lys12) from Western Blots.

Figure 6 The expression of ubiquitin Histone H2A and H2B, and ubiquitin ligase in testis.

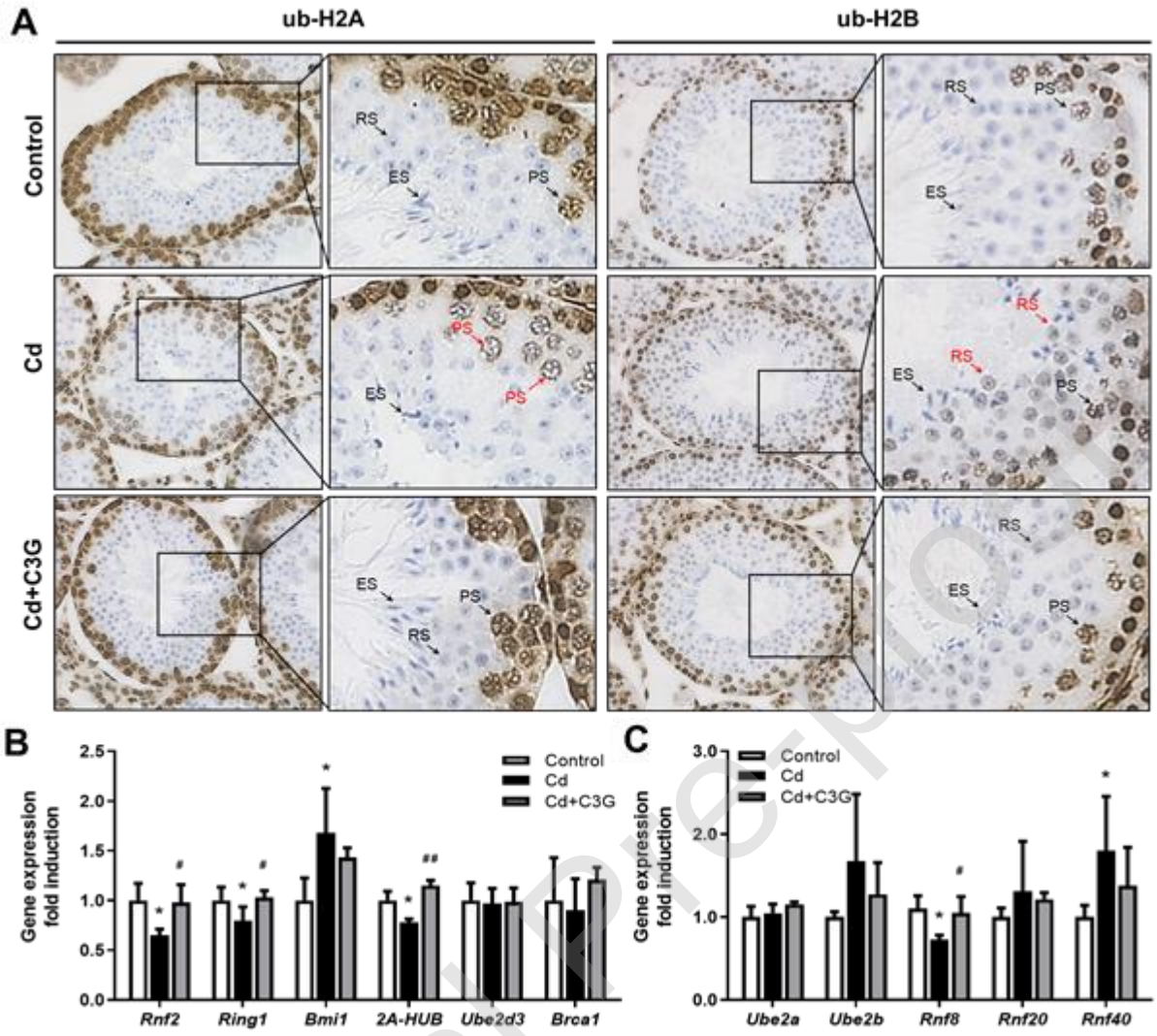

(A) The immunohistochemical analysis of ubiquitin Histone H2A and H2B in the seminiferous tubule at stage Ⅶ-Ⅷ from mice treated for 30 days. RS, Round spermatid; ES, Elongated spermatid; PS, Pachytene spermatocyte; PI, Preleptotene. (B) The expression of mRNA encoding the ubiquitin ligase and ubiquitin-conjugating enzyme participated in the ubiquitination of Histone H2A in testis. (C) The expression of mRNA encoding the ubiquitin ligase and ubiquitin-conjugating enzyme participated in the ubiquitination of Histone H2B in testis. Comparison between all groups was evaluated through One-way ANOVA. Mean±SD. n=4. *p<0.05, **p<0.01, compared with control group. $^{\#}p$<0.05, $^{\#\#}p$<0.01, compared with Cd group.

Figure 7 Measurement of oxidative stress and DNA damage-mediated apoptosis in testis from mice treated for 30 days.

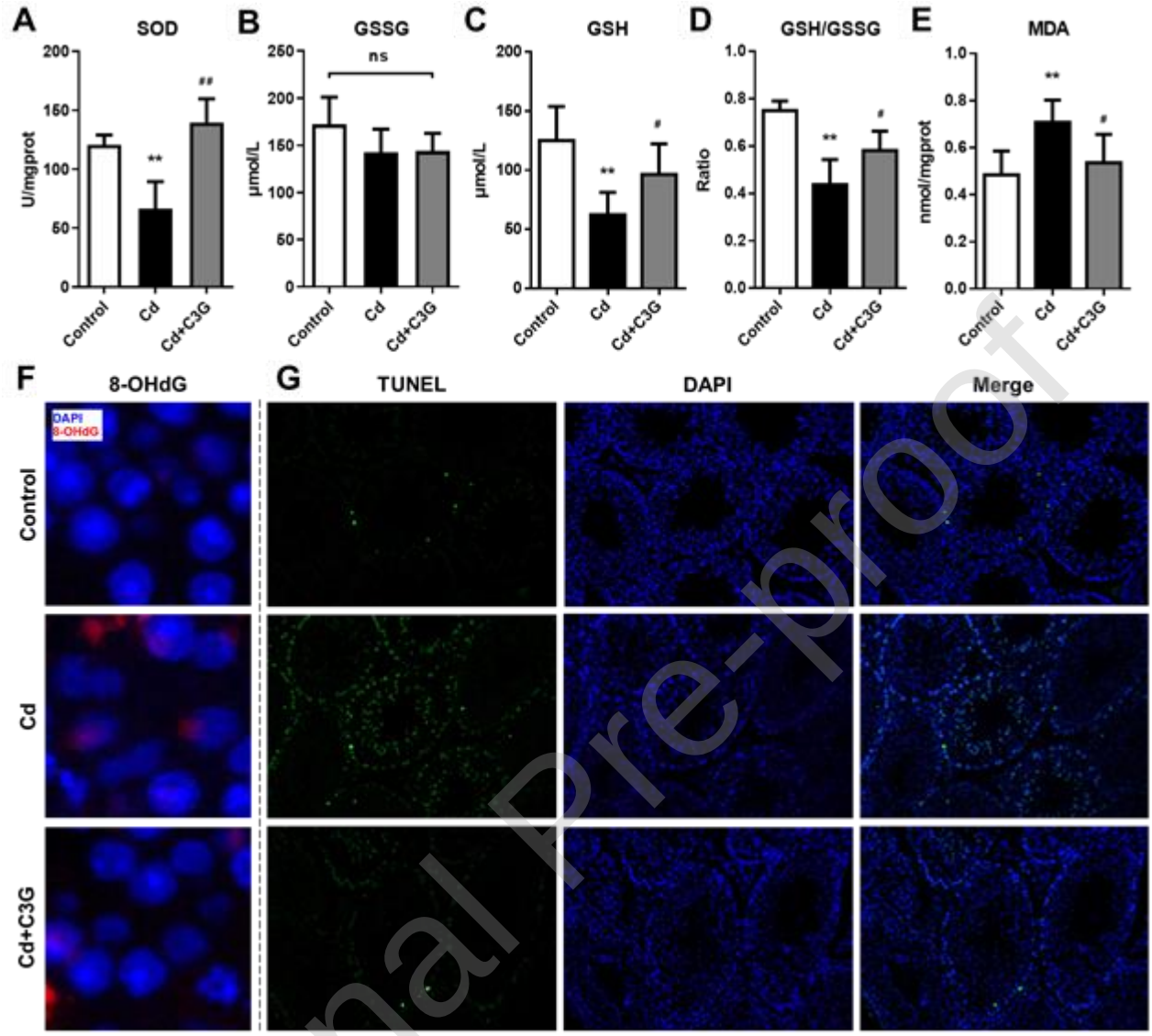

(A) The activity of superoxide dismutase (SOD). (B-D) The level of glutathione (GSH), glutathione disulfide (GSSG), and ratio between GSH and GSSG. (E) The level of MDA. (F) The immunofluorescence analysis of 8-hydroxy-2'-deoxyguanosinein (8-OHdG) in the round spermatids from the testis sections. (G) The assessment of apoptosis in sperm cell from testis sections with TUNEL immunofluorescence. Comparison between all groups was evaluated through One-way ANOVA. Mean±SD. n≥9. $^{**}p<0.01$, compared with control group. $^{\#\#}p<0.01$, $^{\#}p<0.05$, compared with Cd group. ns, not significant.

Figure 8 The expression of protein in testis involved in MAPK signaling pathway.

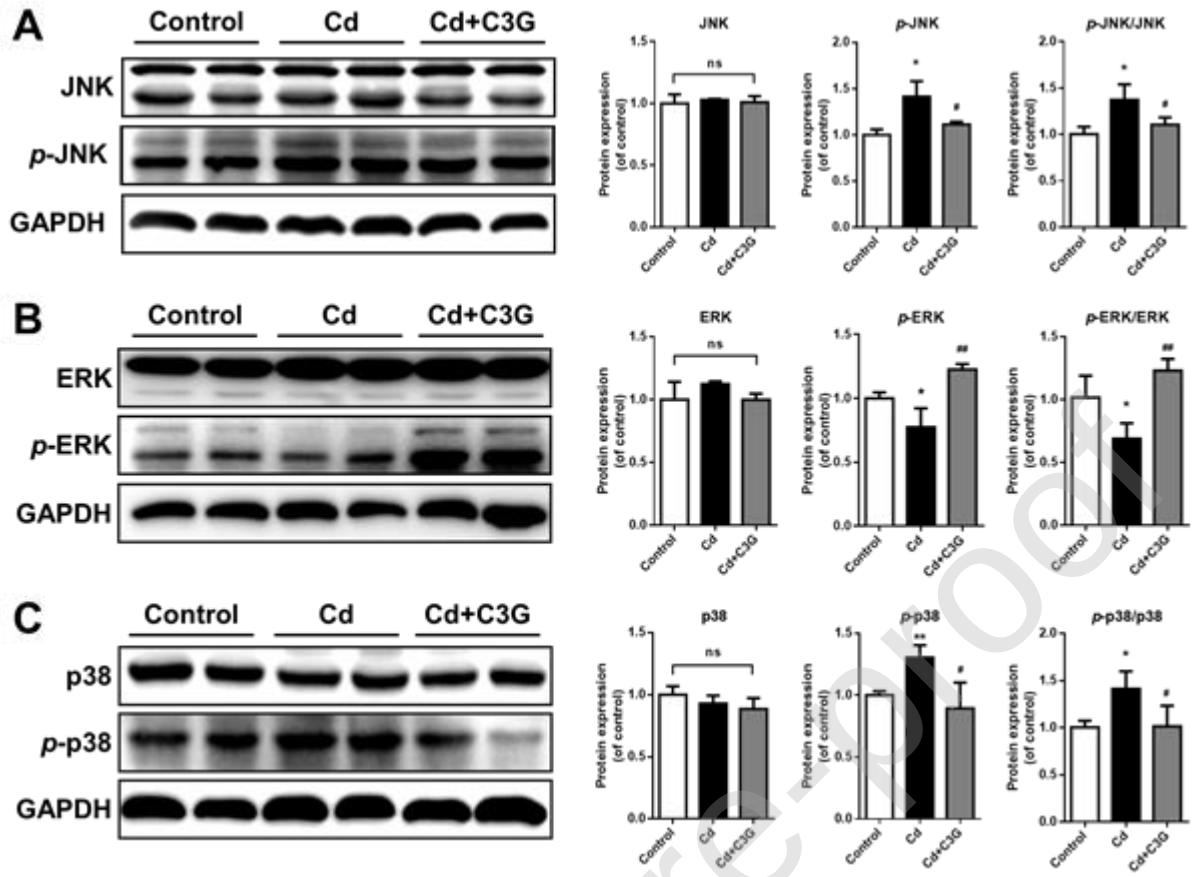

The representative photographs and grayscale analysis of proteins in testis from mice treated for 30 days involved in MAPK signaling pathway. (A) JNK and p-JNK. (B) ERK and p-ERK. (C) p38 and p-p38. Comparison between all groups was evaluated through One-way ANOVA. Mean±SD. n=4. $^{**}p<0.01$, $^{*}p<0.05$, compared with control group. $^{\#\#}p<0.01$, $^{\#}p<0.05$, compared with Cd group. ns, not significant.

Figure 9 The expression of protein in testis involved in mitochondrial apoptosis signaling pathway.

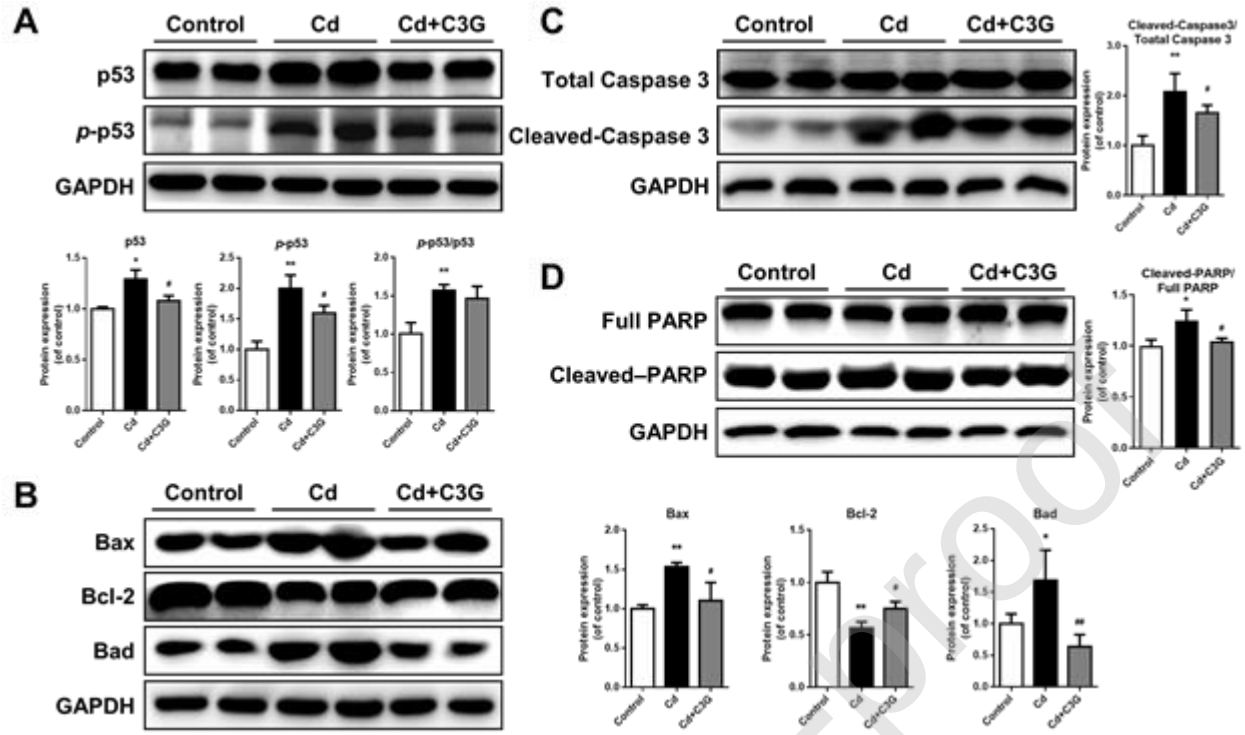

The representative photographs and grayscale analysis of proteins in testis from mice treated for 30 days involved in MAPK signaling pathway. (A) p53 and p-p53. (B) Bax, Bcl-2, and Bad. (C) Total Caspase 3 and Cleaved-Caspase 3. (D) Full PARP and Cleaved-PARP. Comparison between all groups was evaluated through One-way ANOVA. Mean±SD. n=4. $^{**}p<0.01$, $^{*}p<0.05$, compared with control group. $^{\#\#}p<0.01$, $^{\#}p<0.05$, compared with Cd group. ns, not significant.